2025

GPR 3D Image Reconstruction with Sparse Recovery for Random Spatial Sampling

Nihat Alperen Dayanir
University of Vermont

GPR 3D Image Reconstruction with Sparse Recovery for Random Spatial Sampling

A Thesis Presented

by

Nihat Alperen Dayanir

to

The Faculty of the Graduate College

of

The University of Vermont

In Partial Fulfillment of the Requirements
for the Degree of Master of Science
Specializing in Electrical Engineering

January, 2025

Defense Date: November 15th, 2024
Thesis Examination Committee:

Tian Xia, Ph.D., Advisor
Dryver Huston, Ph.D., Chairperson
Jackson Anderson, Ph.D.
Holger Hoock, DPhil, Dean of the Graduate College

Abstract

Ground Penetrating Radar (GPR) is widely used for subsurface exploration in applications such as structural health monitoring, archaeological surveys, and the detection of buried objects. However, traditional 3D GPR imaging requires dense spatial sampling along regular grids, which is time-consuming and often impractical, especially in complex environments with obstacles or accessibility issues.

In this paper, we introduce a novel method that leverages sparse recovery techniques to enhance 3D GPR imaging from reduced spatial measurements collected along arbitrary scanning paths. By exploiting the inherent sparsity of subsurface targets, we employ the Dantzig Selector with cross-validation to accurately reconstruct target locations from spatially random-sampled GPR data.

The reconstructed data is then processed using the Back-Projection Algorithm (BPA) to generate high-resolution 3D images. We validate our method through simulations, demonstrating that our approach not only improves imaging quality but also significantly reduces data acquisition time and storage requirements.

Performance analysis under various noise levels and sampling densities highlights the robustness and practicality of our method for flexible scanning paths in 3D GPR applications. This work contributes to making GPR surveys more efficient and effective, particularly in scenarios where traditional dense sampling is challenging.

Citations

Material from this thesis has been submitted for publication to IEEE International Symposium on Circuits and Systems (ISCAS) on October 13, 2024 in the following form:

- Dayanir, N.A., Huston, D., Xia, T.. "GPR 3D Image Reconstruction for Spatially Sparse Random Sampling" *IEEE International Symposium on Circuits and Systems (ISCAS)*, 2025.

To my family,

with love.

Acknowledgements

First and foremost, I extend my deepest gratitude to my supervisor, Prof. Tian Xia, for his invaluable guidance, insightful feedback, and steadfast encouragement throughout my research journey. Prof. Xia's expertise and thoughtful advice were instrumental in shaping my development as a researcher, providing me with the clarity and direction needed to navigate the challenges of my dissertation work.

I would also like to express my sincere appreciation to my committee members, Prof. Dryver Huston and Prof. Jackson Anderson. Your dedication and the time you devoted to reviewing my work have been invaluable. The depth of your questions and the rigor of your critiques have prompted me to refine my arguments and methodologies, ultimately enhancing the quality of this dissertation.

I owe special thanks to Yan Zhang, for your assistance in understanding the foundations of imaging algorithms. Your help was invaluable.

To my friends, thank you all for the unforgettable moments and joyful distractions along the way. Your humor and companionship have made this journey far more enjoyable, and I will always cherish these memories.

I am deeply grateful to my family-my parents, Ilyas and Fazilet, and my siblings, Rahime, Sinan, and Fatma Nur-. Your patience, motivation, and unwavering belief in me during challenging times have been the cornerstone of my perseverance. Your love and support have given me the strength and confidence to pursue my goals wholeheartedly.

This work was made possible through the YLSY scholarship program by the Ministry of National Education of Türkiye. I am grateful for this incredible opportunity.

In conclusion, I am profoundly thankful to everyone who has contributed to this

journey, directly or indirectly. This thesis stands as a testament not only to my efforts but also to the collective support and guidance I have received. Thank you all for being a part of this pivotal phase of my life.

Table of Contents

List of Figures

Chapter 1

Introduction

1.1 Background and Motivation

Ground Penetrating Radar (GPR) is a non-invasive geophysical method used for subsurface exploration. It operates by emitting electromagnetic pulses into the ground and recording the reflected signals from underground structures or objects. A typical GPR system consists of a transmitter and a receiver, and the collected data are processed to create interpretable subsurface images [1].

GPR data can be visualized using different modes, including A-scan, B-scan, and C-scan. These modes provide one-dimensional, two-dimensional, and three-dimensional representations of the subsurface, respectively. Three-dimensional (3D) imaging significantly enhances GPR's utility by adding spatial context to subsurface features. It enables a more comprehensive understanding of complex underground structures, improving accuracy in tasks such as utility mapping, detection of buried objects, and geological assessments.

However, traditional 3D GPR imaging requires dense spatial sampling over reg-

ular grids, which is often time-consuming and generates large amounts of data. In real-world environments, obstacles or access limitations can complicate grid-based surveys, making such approaches impractical. This necessitates methods capable of reconstructing high-quality 3D images from sparse, irregularly sampled data.

1.2 Problem Statement

While sparse recovery techniques have shown promise in GPR imaging, challenges remain in effectively integrating these methods with arbitrary path scanning. Existing algorithms often rely on regular sampling and struggle with irregularly sampled data, limiting their application in complex environments where such paths are necessary.

There is a need for a robust framework that can handle arbitrary scanning paths and fully exploit the sparsity in three-dimensional GPR imaging. Such a framework would significantly reduce data acquisition time and storage requirements while maintaining or improving imaging quality.

1.3 Research Objectives

The main objectives of this research are:

1. **Develop a robust sparse recovery framework** tailored for arbitrary path GPR scanning that can reconstruct high-quality 3D images from sparsely and irregularly sampled data.

2. **Validate the effectiveness of the proposed method** through simulations involving various noise levels and sampling densities using realistic GPR models.

3. **Demonstrate the practical benefits** of flexible scanning paths in real-world environments where regular grids are impractical due to obstacles or accessibility constraints.

1.4 Thesis Structure

The thesis is organized as follows:

- **Chapter 2: Literature Review** — Provides a comprehensive review of GPR imaging techniques, sparse recovery methods, and their applications in GPR, highlighting the limitations of existing methods.
- **Chapter 3: Methodology** — Presents the theoretical foundation and methodology of the proposed sparse recovery framework and back-projection algorithm (BPA) for GPR imaging, including the construction of the data dictionary and the implementation of the Dantzig Selector with cross-validation.
- **Chapter 4: Results and Discussion** — Details the implementation of the proposed method, presents the simulation results, and provides a comparative analysis with traditional imaging methods.
- **Chapter 5: Conclusion and Future Work** — Summarizes the key findings, discusses the implications of the research, and suggests directions for future studies.

Chapter 2

Literature Review

2.1 Ground Penetrating Radar Imaging Techniques

Ground Penetrating Radar (GPR) is a geophysical method that uses radar pulses to image the subsurface [2]. It is widely used in applications such as civil engineering, archaeology, and geological surveys [3]. GPR systems emit electromagnetic waves into the ground and record the reflected signals from subsurface structures to construct images.

Traditional GPR imaging requires dense spatial sampling along regular grids to produce high-resolution three-dimensional (3D) images [4]. The data acquisition process involves collecting GPR data at closely spaced intervals, which can be time-consuming and impractical in complex environments.

Several imaging techniques are commonly employed in GPR data processing to accurately visualize subsurface structures. These techniques address the need to

correct wave propagation effects, repositioning reflected signals to reconstruct clear images of subsurface features.

2.1.1 Migration Techniques

Migration algorithms in GPR aim to correct the spatial displacement of reflected signals caused by wave propagation, thereby producing more accurate images of the subsurface [5]. Common migration methods in GPR include:

- **Kirchhoff Migration**: A time-domain method known for its flexibility in handling complex subsurface structures [6].
- **Stolt Migration**: A frequency-domain method that is efficient but generally assumes a constant velocity medium [5].
- **Back-Projection Algorithm (BPA)**: Although originally developed for Synthetic Aperture Radar (SAR), BPA has been adapted as a migration technique in GPR [7–9]. BPA reconstructs subsurface images by back-projecting recorded signals onto a spatial grid, taking into account the varying travel times and distances between the antenna and each subsurface point [10].

2.1.2 Synthetic Aperture Radar (SAR) Techniques in GPR

SAR techniques, which were originally designed for airborne or satellite radar systems, synthesize a larger antenna aperture by moving a smaller antenna over the target area [11]. This approach enhances spatial resolution in imaging. In GPR applications,

SAR techniques, including the Back-Projection Algorithm (BPA), have been adapted to achieve high-resolution subsurface images [7].

2.1.3 Back-Projection Algorithm (BPA): Migration and SAR Origins

The Back-Projection Algorithm (BPA) holds a dual role in GPR: it is recognized both as a migration technique [9] and as a method originating from SAR [8]. In the context of GPR, BPA is applied as a migration algorithm to reconstruct subsurface images by repositioning reflected energy based on varying travel times. Due to BPA's adaptability, it can process data collected along non-uniform or synthetic apertures, making it valuable in applications that involve irregular sampling or flexible scan paths.

2.1.4 Limitations of Traditional GPR Imaging

Traditional GPR imaging techniques generally rely on dense, regular sampling to ensure high-resolution images. However, in real-world scenarios, achieving such sampling density can be impractical due to physical obstacles, limited access, and time constraints [12]. This limitation highlights the need for advanced methods capable of reconstructing accurate images from sparse or irregularly sampled data, as addressed in this thesis through sparse recovery techniques.

2.2 Sparse Recovery Techniques

Sparse recovery, also known as compressed sensing, is a signal processing technique that reconstructs signals from a small number of measurements by exploiting the sparsity of the signal [13, 14]. In many practical applications, including GPR, the underlying signal can be represented using a sparse set of basis functions.

2.2.1 Compressed Sensing Theory

Compressed sensing theory states that a sparse signal can be recovered from a small number of linear measurements, provided that certain conditions are met [13]. The recovery is typically formulated as an optimization problem:

$$\min_{\mathbf{x}} \|\mathbf{x}\|_1 \quad \text{subject to} \quad \mathbf{y} = \mathbf{\Phi x}, \tag{2.1}$$

where $\mathbf{x}$ is the sparse signal, $\mathbf{y}$ is the measurement vector, and $\mathbf{\Phi}$ is the measurement matrix.

2.2.2 Sparse Representation in GPR Imaging

In GPR imaging, the subsurface often contains a few discrete targets within a larger volume, making the reflectivity function sparse [12]. By constructing a suitable dictionary that models the GPR responses from potential target locations, sparse recovery techniques can be applied to estimate the subsurface image from incomplete data.

2.3 Previous Work on Sparse GPR Imaging

Gurbuz *et al.* introduced the application of compressed sensing to GPR imaging, demonstrating that high-quality images can be reconstructed from significantly fewer measurements [12, 15]. They utilized random spatial sampling and sparse recovery algorithms to reconstruct the subsurface reflectivity, reducing data acquisition time and computational load.

Herman and Strohmer applied compressed sensing to synthetic aperture radar (SAR) imaging, which shares similarities with GPR, showing improved imaging performance with reduced data [16]. Their work highlights the potential of compressed sensing in radar imaging applications where data acquisition is costly or limited.

Zhang and Xia explored frequency-domain clutter removal techniques for compressive GPR, enabling more flexible data acquisition and improved imaging in challenging environments [17]. Their method addresses the issue of clutter in GPR data, which can obscure target reflections.

Frigui et al. [18] focused on the application of sparse recovery techniques for landmine detection using GPR data. They developed algorithms that leverage sparse representation and feature extraction to improve detection accuracy and reduce false alarms. By modeling the landmine signatures as sparse components within the GPR signals, their approach enhances the discrimination between landmines and clutter. This work demonstrates the effectiveness of sparse recovery methods in practical and critical applications, further showcasing the versatility of these techniques in GPR

imaging.

2.4 Dantzig Selector in Sparse Recovery

The Dantzig Selector is an estimator designed for statistical estimation in high-dimensional linear models where the number of parameters exceeds the number of observations [19]. It is particularly effective in sparse recovery problems where the underlying signal has a sparse representation.

In the context of compressed sensing and GPR imaging, the Dantzig Selector offers the following advantages:

- **Robust Sparse Recovery**: Provides stable recovery of sparse signals even in the presence of noise.
- **Computational Efficiency**: The optimization problem can be formulated as a linear program, which is computationally tractable.

2.4.1 Applications in GPR Imaging

While the Dantzig Selector has been extensively studied in statistics and signal processing, its application to GPR imaging is an emerging area. Gurbuz et al. [12] applied the Dantzig Selector for high-resolution GPR imaging, demonstrating improved reconstruction quality in noisy measurements.

2.5 Back-Projection Algorithm in GPR Imaging

The Back-Projection Algorithm (BPA) is a classical approach used to reconstruct spatial information from GPR signals. BPA works by mapping received radar signals back into the spatial domain, producing images that reveal the location of underground targets. However, BPA assumes uniformly sampled data and struggles with irregular or sparse sampling, leading to imaging artifacts in such cases [7].

2.6 Limitations of Existing Methods

While previous studies have successfully applied sparse recovery to GPR imaging, they often assume regular or structured sampling patterns or focus on two-dimensional imaging. Additionally, many methods do not accommodate arbitrary scanning paths, limiting their applicability in complex environments where such paths are necessary. There is a need for methods that can handle arbitrary scanning paths and three-dimensional imaging with sparse and irregular spatial sampling.

2.7 Summary

The literature indicates that sparse recovery techniques have the potential to significantly improve GPR imaging by reducing data acquisition requirements and handling incomplete data. However, challenges remain in extending these methods to accom-

modate arbitrary scanning paths and fully exploit the sparsity in three-dimensional GPR imaging. This thesis aims to address these challenges by developing a sparse recovery framework suitable for spatially sparse random sampling along arbitrary paths.

Chapter 3

Methodology

3.1 Sparse Recovery Framework for GPR Imaging

3.1.1 Overview of Sparse Recovery Techniques

Sparse recovery techniques are mathematical methods used to reconstruct signals or images from incomplete or undersampled data by leveraging the inherent sparsity in the signal domain. In many practical applications, including GPR imaging, the underlying signal or image can be represented using a small number of non-zero coefficients in an appropriate basis or dictionary.

Principles of Sparse Representation

The concept of sparsity revolves around the idea that a signal $\mathbf{x} \in \mathbb{R}^N$ can be represented as a linear combination of a small number of elements from a basis or dictionary

$\mathbf{\Psi} \in \mathbb{R}^{N \times K}$:

$$\mathbf{x} = \mathbf{\Psi s}, \tag{3.1}$$

where $\mathbf{s} \in \mathbb{R}^K$ is a sparse coefficient vector with $\|\mathbf{s}\|_0 = S \ll N$.

In signal acquisition, we often measure a set of linear projections $\mathbf{y} \in \mathbb{R}^M$ of the signal $\mathbf{x}$:

$$\mathbf{y} = \mathbf{\Phi x} + \mathbf{n}, \tag{3.2}$$

where $\mathbf{\Phi} \in \mathbb{R}^{M \times N}$ is the measurement matrix, and $\mathbf{n} \in \mathbb{R}^M$ represents measurement noise. When $M < N$, this system is underdetermined, and traditional reconstruction methods cannot uniquely recover $\mathbf{x}$.

Compressed Sensing Theory

Compressed sensing (CS) theory addresses the problem of recovering sparse signals from an underdetermined set of linear measurements. It asserts that if the signal $\mathbf{x}$ is sparse or compressible in some basis, it can be recovered from far fewer samples than traditionally required [14]. The recovery of $\mathbf{s}$ from $\mathbf{y}$ can be formulated as an optimization problem:

$$\min_{\mathbf{s}} \|\mathbf{s}\|_1 \quad \text{subject to} \quad \mathbf{y} = \mathbf{\Phi\Psi s}. \tag{3.3}$$

Application to GPR Imaging

In traditional sparse recovery, a measurement matrix $\mathbf{\Phi}$ is used if the measured signal is below the Nyquist rate. In our work, however, the measured signal meets the Nyquist criterion, providing all necessary samples without dimensionality reduction. Consequently, we bypass $\mathbf{\Phi}$ and instead use a dictionary matrix $\mathbf{\Psi}$ that directly models spatial target reflections, allowing us to reconstruct the sparse target reflectivity vector $\mathbf{b}$ in full resolution.

3.1.2 Constructing the GPR Data Dictionary

GPR transmissions over a region of interest form a synthetic aperture, resulting in an impulse response that follows a spatially variant curve in the space-time domain. The received signal at the antenna, reflected from a point target at position $\mathbf{P}$, is a time-delayed and scaled version of the transmitted signal $s(t)$. This can be modeled as:

$$\beta_i(t) = As\left(t - \tau_i(\mathbf{P})\right), \tag{3.4}$$

where $\tau_i(\mathbf{P})$ is the total round-trip delay between the transmitter and the target at position $\mathbf{P}$ for the i-th aperture point, and A is a scaling factor accounting for signal spreading and amplitude attenuation.

The total travel time $\tau_i(\mathbf{P})$ depends on the distances traveled in different media and their respective wave velocities:

$$\tau_i(\mathbf{P}) = \frac{d_1 + d_4}{v_1} + \frac{d_2 + d_3}{v_2}, \tag{3.5}$$

where d_1 through d_4 are distances as illustrated in Figure 3.1, and v_1 and v_2 are the wave velocities in the respective media.

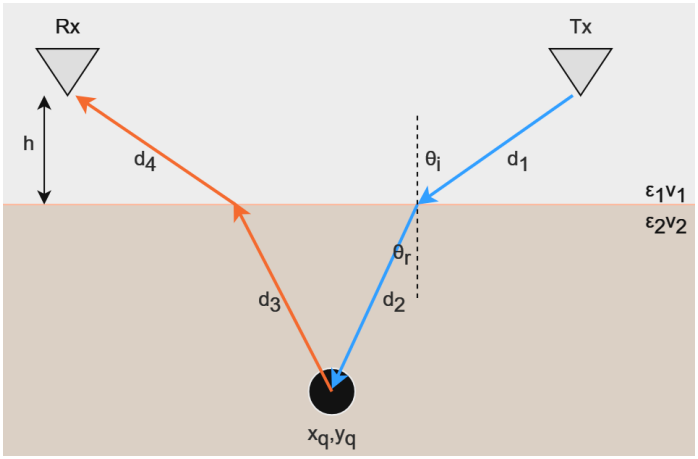

Figure 3.1: GPR setup showing a bistatic configuration with path distances for travel time calculation.

To construct the dictionary $\mathbf{\Psi}$, we discretize the target space Π_T, defined within the bounds $[x_i, x_f] \times [y_i, y_f] \times [z_i, z_f]$. This discretization generates a set of N target points $\{\boldsymbol{\pi}_1, \boldsymbol{\pi}_2, \ldots, \boldsymbol{\pi}_N\}$, where each $\boldsymbol{\pi}_j = [x_j, y_j, z_j]$ is a 3D coordinate. The resolution of the dictionary is determined by the number of discretization points N.

For each scan position i and each target point $\boldsymbol{\pi}_j$, we compute the time delay $\tau_i(\boldsymbol{\pi}_j)$ using Equation (3.5). The j-th column of the $N_t \times N$ matrix $\mathbf{\Psi}_i$ is then constructed as:

$$[\mathbf{\Psi}_i]_j = \frac{s\left(t - \tau_i(\boldsymbol{\pi}_j)\right)}{\left\| s\left(t - \tau_i(\boldsymbol{\pi}_j)\right)\right\|_2}, \quad t = t_0, t_0 + \tfrac{1}{F_s}, \ldots, t_0 + \tfrac{N_t - 1}{F_s}, \tag{3.6}$$

where F_s is the sampling frequency, t_0 is the initial time, and N_t is the number of time samples. Normalizing each column to have unit ℓ_2 norm ensures numerical stability in the reconstruction process.

3.1.3 Formulation of the Sparse Recovery Problem

The observed data vector at scan position i is:

$$\boldsymbol{\beta}_i = \left[\beta_i(t_0), \beta_i\left(t_0 + \tfrac{1}{F_s}\right), \ldots, \beta_i\left(t_0 + \tfrac{N_t-1}{F_s}\right)\right]^\top \in \mathbb{R}^{N_t}. \tag{3.7}$$

Assuming linearity, the relationship between the observed data and the target reflectivity vector $\mathbf{b}$ is given by:

$$\boldsymbol{\beta}_i = \boldsymbol{\Psi}_i \mathbf{b}, \tag{3.8}$$

where $\mathbf{b} = [b_1, b_2, \ldots, b_N]^\top$ is the reflectivity vector of the target space, with non-zero entries indicating the presence of targets at the corresponding discretized locations.

By stacking the observed data and dictionaries from all M scan positions, we form:

$$\beta = \begin{bmatrix} \boldsymbol{\beta}_1 \\ \boldsymbol{\beta}_2 \\ \vdots \\ \boldsymbol{\beta}_M \end{bmatrix}, \quad \Psi = \begin{bmatrix} \boldsymbol{\Psi}_1 \\ \boldsymbol{\Psi}_2 \\ \vdots \\ \boldsymbol{\Psi}_M \end{bmatrix} \tag{3.9}$$

The sparse recovery problem aims to reconstruct $\mathbf{b}$ from β by solving:

$$\min_{\mathbf{b}} \|\mathbf{b}\|_1 \quad \text{subject to} \quad \beta = \Psi \mathbf{b}. \tag{3.10}$$

In practice, due to measurement noise and modeling inaccuracies, we consider a relaxed version:

$$\min_{\mathbf{b}} \|\mathbf{b}\|_1 \quad \text{subject to} \quad \|\beta - \Psi\mathbf{b}\|_2 \leq \epsilon, \tag{3.11}$$

where ϵ is a parameter reflecting the noise level.

Alternatively, we can use the Dantzig Selector formulation [19] for robust recovery in the presence of noise:

$$\min_{\mathbf{b}} \|\mathbf{b}\|_1 \quad \text{subject to} \quad \|\Psi^\top(\beta - \Psi\mathbf{b})\|_\infty \leq \epsilon. \tag{3.12}$$

3.1.4 Placement Matrix for Merging Observed Data

In random spatial sampling, the observed data matrix β_{random} corresponds to measurements taken at i random scan points, which do not align with the M grid positions defined by the dictionary matrix Ψ. This mismatch prevents direct application of sparse recovery algorithms.

To address this issue, we introduce the **placement matrix** $\Xi \in \mathbb{R}^{M\times i}$, which maps the random scan points to the desired grid positions. Ξ is defined as:

$$\Xi_{jk} = \begin{cases} 1, & \text{if the } k\text{-th random scan point corresponds to the } j\text{-th grid position,} \\ 0, & \text{otherwise.} \end{cases} \tag{3.13}$$

Impact on Observed Data

The placement matrix rearranges the observed data $\beta_{\text{random}} \in \mathbb{R}^i$ into the merged observed data $\beta_{\text{merged}} \in \mathbb{R}^M$, aligned with the grid positions in Ψ, as follows:

$$\beta_{\text{merged}} = \Xi^\top \beta_{\text{random}}. \tag{3.14}$$

Sparse Recovery Problem

With the merged observed data β_{merged}, the sparse recovery problem is formulated as:

$$\min_{\mathbf{b}} \|\mathbf{b}\|_1 \quad \text{subject to} \quad \|\beta_{\text{merged}} - \Psi\mathbf{b}\|_2 \leq \epsilon, \tag{3.15}$$

where:

- $\Psi \in \mathbb{R}^{N \times N}$ is the dictionary matrix representing the full grid.
- $\mathbf{b} \in \mathbb{R}^N$ is the sparse reflectivity vector of the subsurface.
- ϵ accounts for noise in the observations.

Construction of the Placement Matrix

To construct Ξ:

1. Identify the correspondence between the i random scan points and the M grid positions.
2. For each grid position j and random scan point k, set $\Xi_{jk} = 1$ if the k-th scan point aligns with the j-th grid position; otherwise, set $\Xi_{jk} = 0$.

3. Ensure Ξ is of size $M \times i$, where M is the total number of grid positions and i is the number of random scan points.

Advantages of the Placement Matrix

The placement matrix ensures that the randomly sampled observed data β_{random} can be merged into a format compatible with the dictionary matrix Ψ, enabling accurate reconstruction of the sparse reflectivity vector $\mathbf{b}$ using the sparse recovery framework.

3.1.5 Implementation of the Dantzig Selector with Cross-Validation

The choice of the parameter ϵ in Equation (3.12) is critical. An improper choice may lead to overfitting (introducing false targets) or underfitting (missing true targets). To select an appropriate ϵ, we use a cross-validation (CV) approach:

1. **Data Partitioning**: Split the data into an estimation set $\beta_{\mathcal{E}}$ and a cross-validation set β_{cv}.

2. **Initialization**: Set $\varepsilon = \alpha \|\Psi_{\mathcal{E}}^{\top} \beta_{\mathcal{E}}\|_{\infty}$, $\hat{\mathbf{b}} = 0$, and $i = 1$. An initial ε that allows the method not to overfit the data can be selected by setting $\alpha = 0.99$. Note that for $\alpha > 1$, we would get $\hat{\mathbf{b}} = 0$ as the minimum ℓ_1 norm solution.

3. **Estimation**: Solve the optimization problem:

$$\hat{\mathbf{b}}^{(i)} = \arg\min_{\mathbf{b}} \|\mathbf{b}\|_1 \quad \text{subject to} \quad \|\Psi_{\mathcal{E}}^{\top}(\beta_{\mathcal{E}} - \Psi_{\mathcal{E}}\mathbf{b})\|_{\infty} \leq \epsilon. \tag{3.16}$$

4. **Cross-Validation Check**: Compute the cross-validation residual:

$$\varepsilon_{\text{cv}} = \|\Psi_{\text{cv}}^{\top}(\beta_{\text{cv}} - \Psi_{\text{cv}}\hat{\mathbf{b}}^{(i)})\|_{\infty}. \tag{3.17}$$

If $\varepsilon_{\text{cv}} < \epsilon$, update $\epsilon = \varepsilon_{\text{cv}}$, increment i, and return to Step 3. Otherwise, terminate the algorithm.

3.2 Back-Projection Algorithm

The Back-Projection Algorithm (BPA) is a commonly used imaging technique in GPR data processing,. BPA simplifies radar-reflected wave interpretation by back-projecting the received signals onto the spatial domain, effectively mapping reflections to their potential source locations.

Originally developed for synthetic aperture radar [20], BPA calculates the propagation time of electromagnetic waves from the transmitting antenna to a reflection point and back to the receiver. For each scan position k and each point $\mathbf{P}_i$ in the subsurface domain, the travel time $\tau_{i,k}$ is computed. The received signal at time $\tau_{i,k}$ is associated with the point $\mathbf{P}_i$.

The imaging value at point $\mathbf{P}_i$ is obtained by summing the contributions from all scan positions:

$$I(\mathbf{P}_i) = \sum_{k=1}^{M} g(\theta_{i,k}) s_k(\tau_{i,k}), \tag{3.18}$$

where $s_k(t)$ is the received signal or reconstructed signal from multiplying $\mathbf{\Psi}$ and found $\mathbf{b}$ at scan position k, $\theta_{i,k}$ is the angle between the z-axis and the line from the

receiver to $\mathbf{P}_i$, and $g(\theta_{i,k})$ is a gain function that compensates for angular dependence.

3.3 Summary

In this chapter, we presented the methodology for enhancing 3D GPR imaging using sparse recovery techniques. We began with an overview of sparse recovery principles and their application to GPR imaging, emphasizing the construction of a data dictionary that models the spatial target reflections. We formulated the sparse recovery problem using the Dantzig Selector and introduced a cross-validation approach for parameter selection to ensure robust reconstruction in the presence of noise.

Additionally, we described the Back-Projection Algorithm as a conventional imaging method, a method for 3D image reconstruction. We highlighted its limitations when applied to sparsely and irregularly sampled data, reinforcing the need for advanced methods like sparse recovery to achieve high-quality imaging in challenging environments.

Chapter 4

Results and Discussion

4.1 Introduction

In this chapter, we present the results of applying the proposed sparse recovery framework to enhance 3D GPR imaging from sparsely and irregularly sampled data collected along arbitrary scanning paths. We validate the effectiveness of our method through comprehensive simulations using the gprMax electromagnetic simulation tool. The performance of the sparse recovery approach is evaluated under various sampling densities and noise levels, and comparisons are made with traditional imaging and interpolation methods. The impact of the cross-validation parameter on reconstruction accuracy is also examined.

4.2 Simulation Setup

4.2.1 GPR Model and Configuration

To simulate realistic GPR data, we employed gprMax [21], an open-source finite-difference time-domain (FDTD) electromagnetic simulation software. The simulations were designed to mimic a typical GPR survey with the following specifications:

- **Antenna Configuration**: A bistatic antenna setup was used, with a transmitter-receiver separation of 0.04 meters. This configuration is common in practical GPR systems and allows for effective target detection.
- **Operating Frequency**: The system operated at a central frequency of 1.5 GHz, utilizing a Ricker waveform as the transmitted pulse. This frequency provides a good balance between penetration depth and resolution for subsurface imaging.
- **Target Space**: The simulation domain spanned 0.65 meters in length (X-axis), 0.40 meters in width (Z-axis), and 0.12 meters in depth (Y-axis). Three buried objects were placed within this domain at varying depths and positions to represent typical subsurface targets (Figure 4.1).

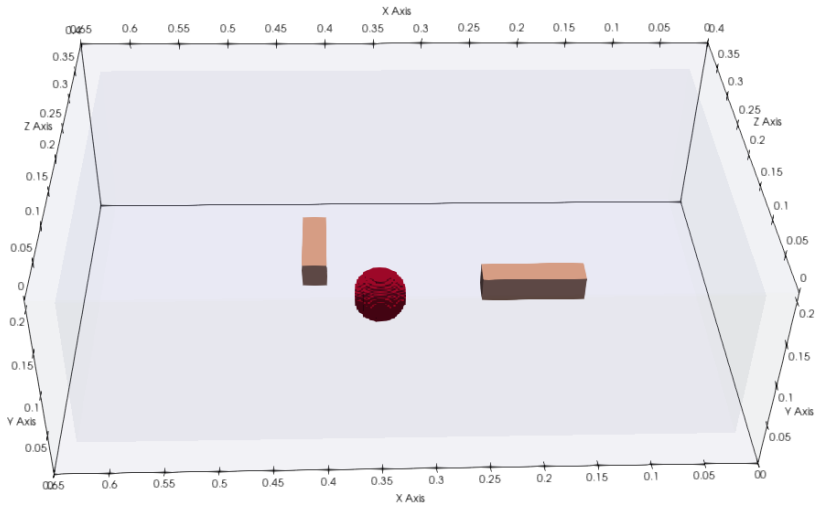

Figure 4.1: Simulated GPR setup showing the bistatic measurement configuration and target locations.

4.2.2 Data Acquisition and Sampling Strategy

A complete C-scan survey was performed over the target space, moving the antenna system along a regular grid with a step size of 0.02 meters in both the X and Z directions. This resulted in a total of 486 A-scans, providing comprehensive coverage of the subsurface area.

To emulate sparse and irregular sampling along arbitrary paths, subsets of the full dataset were randomly selected. Sampling percentages of 10%, 20%, 30%, 40%, and 50% of the full dataset were considered. For each sampling rate, the selection process was repeated five times to account for the randomness in the sampling pattern, ensuring that the results were statistically significant.

4.2.3 Noise Addition

To simulate real-world measurement conditions, Gaussian noise was added to the GPR data at varying signal-to-noise ratios (SNRs). The SNR levels ranged from -25 dB to 15 dB. This range encompasses scenarios from extremely noisy environments to relatively clean measurements, allowing us to assess the robustness of the proposed method under different noise conditions.

4.3 Sparse Recovery and Imaging Results

4.3.1 Observation Vector and Dictionary Matrix Sizes

The complete dataset consisted of A-scan data collected at all 486 scan points, with each A-scan containing 52 time samples. The resulting vectorized observation and reflectivity matrices had the following sizes:

- **Observation Vector, $\boldsymbol{\beta}$**: $(52 \times 486) \times 1$, where 52 corresponds to the number of time samples per scan point, and 486 corresponds to the total scan points.
- **Reflectivity Vector, $\mathbf{b}$**: $(52 \times 486) \times 1$, representing the sparsity of the reflectivity values across the entire image domain.
- **Dictionary Matrix, $\boldsymbol{\Psi}_{\mathbf{total}}$**: $(52 \times 486) \times (52 \times 486)$, representing the entire image domain. This matrix captures the relationship between the reflectivity vector $\mathbf{b}$ and the observed data $\boldsymbol{\beta}$ across all scan positions.

To emulate sparse and irregular sampling along arbitrary paths, subsets of the full dataset were randomly selected. Sampling percentages of 10%, 20%, 30%, 40%, and 50% of the full dataset were considered. For example:

- For 10% sampling, $0.1 \times 486 = 49$ random scan points were selected, resulting in an observation vector $\boldsymbol{\beta}_{\text{random}}$ of size $(52 \times 49) \times 1$.
- For 50% sampling, $0.5 \times 486 = 243$ scan points were selected, resulting in $\boldsymbol{\beta}_{\text{random}}$ of size $(52 \times 243) \times 1$.

4.3.2 Constructing $\boldsymbol{\beta}_{\text{MERGED}}$ Using the Placement Matrix

To align the randomly sampled observation vector $\boldsymbol{\beta}_{\text{random}}$ with the sparse recovery framework, a placement matrix $\boldsymbol{\Xi}$ is used. The placement matrix has dimensions:

$$\boldsymbol{\Xi} \in \mathbb{R}^{(52\times 486)\times(52\times n_{\text{samples}})},$$

where n_{samples} is the number of randomly selected scan points.

The merged observation vector $\boldsymbol{\beta}_{\text{merged}}$ is obtained as:

$$\boldsymbol{\beta}_{\text{merged}} = \boldsymbol{\Xi}^{\top} \boldsymbol{\beta}_{\text{random}},$$

with $\boldsymbol{\beta}_{\text{merged}}$ having dimensions $(52 \times 486) \times 1$, making it compatible with the framework.

4.3.3 Constructing $\mathbf{\Psi}_{\text{TOTAL}}$ from Individual $\mathbf{\Psi}_i$

The dictionary matrix $\mathbf{\Psi}_{\text{total}}$ is constructed by stacking individual dictionary matrices $\mathbf{\Psi}_i$ corresponding to each scan point. Each $\mathbf{\Psi}_i$ models the time-delayed response for a given scan point and has dimensions:

$$\mathbf{\Psi}_i \in \mathbb{R}^{52\times(52\times 486)}.$$

For all 486 scan points, $\mathbf{\Psi}_{\text{total}}$ is constructed as:

$$\mathbf{\Psi}_{\text{total}} = \begin{bmatrix} \mathbf{\Psi}_1 \\ \mathbf{\Psi}_2 \\ \vdots \\ \mathbf{\Psi}_{486} \end{bmatrix},$$

resulting in a matrix of size $(52 \times 486) \times (52 \times 486)$.

This stacking process ensures that the dictionary captures the contributions from all scan points in the desired image domain, enabling the sparse recovery framework to reconstruct the entire reflectivity vector $\mathbf{b}$.

4.3.4 Application of the Sparse Recovery Framework

The sparse recovery framework was applied to the merged observation vector $\boldsymbol{\beta}_{\text{merged}}$. The Dantzig Selector formulation with cross-validation, as detailed in Chapter 3, was used to estimate the sparse reflectivity vector $\mathbf{b}$.

4.3.5 Reconstruction of Subsurface Images

The reconstructed dataset, obtained by multiplying the estimated $\mathbf{b}$ with the dictionary matrix $\mathbf{\Psi}_{\text{total}}$, was processed using the Back-Projection Algorithm (BPA) to generate high-resolution 3D images of the subsurface.

4.3.6 Application of the Sparse Recovery Framework

The randomly sampled and noisy GPR data were processed using the proposed sparse recovery framework. The Dantzig Selector formulation with cross-validation, as detailed in Chapter 3, was employed to estimate the sparse reflectivity vector $\mathbf{b}$. The optimization problem was solved using the CVX package for convex optimization [22], ensuring numerical stability and efficiency.

4.3.7 Reconstruction of Subsurface Images

Once the sparse reflectivity vector $\mathbf{b}$ was obtained, the missing data in the spatial domain were reconstructed by multiplying the found $\mathbf{b}$ with $\mathbf{\Psi}$. The reconstructed dataset was then processed using the Back-Projection Algorithm (BPA) to generate high-resolution 3D images of the subsurface.

4.3.8 Comparison with Traditional Imaging

To highlight the effectiveness of the sparse recovery approach, we compared the imaging results with those obtained by directly applying BPA to the randomly sampled data without any reconstruction. Figure 4.2 illustrates this comparison for the case of 30% sampling with an SNR of 5 dB.

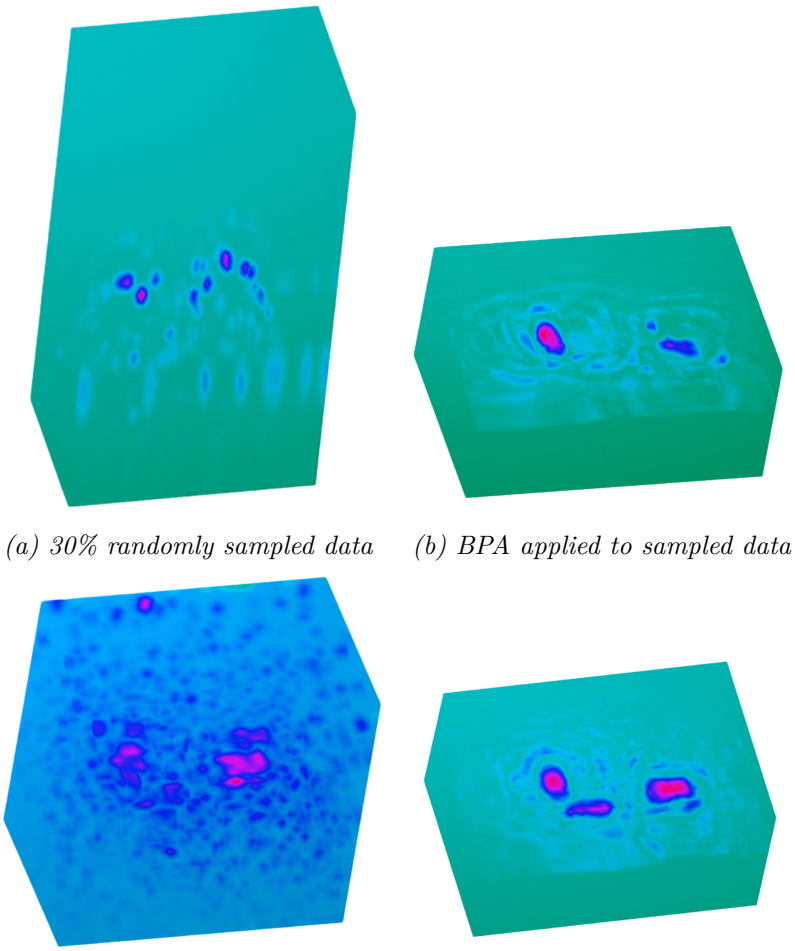

(a) 30% randomly sampled data

(b) BPA applied to sampled data

(c) Reconstructed data using sparse recovery

(d) BPA applied to reconstructed data

Figure 4.2: Imaging results for 30% sampling with 5 dB noise: (a) Randomly sampled data, (b) BPA on sampled data, (c) Data reconstructed using sparse recovery, (d) BPA on reconstructed data.

As shown in Figure 4.2b, applying BPA directly to the sparsely sampled data resulted in poor image quality, with significant artifacts and missing target information due to the irregular and incomplete sampling. In contrast, Figure 4.2d demonstrates that the sparse recovery approach effectively reconstructed the missing data, enabling BPA to produce a clear and accurate 3D image of the subsurface targets.

4.4 Performance Analysis

4.4.1 Mean Squared Error Evaluation

To quantitatively assess the performance of the proposed method, we calculated the Mean Squared Error (MSE) between the reconstructed images and the ground truth images obtained from the full dataset without noise. The MSE provides a measure of the reconstruction accuracy, with lower values indicating better performance.

Figure 4.3 shows the MSE as a function of the SNR for different sampling percentages. The results indicate that the sparse recovery method maintains low MSE values even at reduced sampling rates and lower SNRs, demonstrating robustness to both sparse sampling and noise.

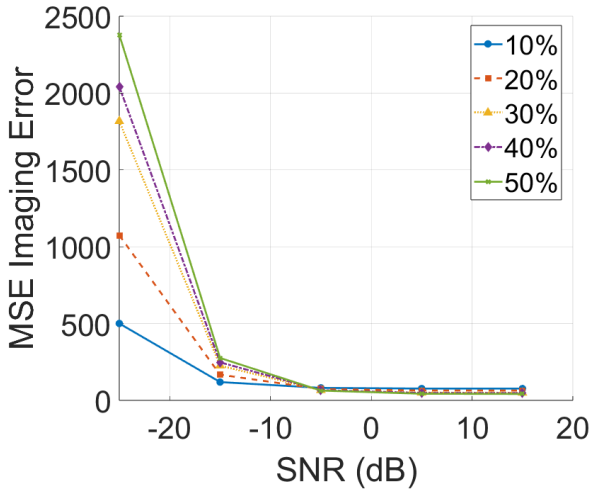

Figure 4.3: Mean Squared Error (MSE) versus Signal-to-Noise Ratio (SNR) for different sampling percentages using the proposed sparse recovery method.

4.4.2 Comparison with Traditional Interpolation Methods

To further validate the effectiveness of the sparse recovery approach, we compared it with traditional interpolation methods commonly used to fill missing data in GPR imaging:

- **Nearest Neighbor Interpolation**
- **Linear Interpolation**
- **Cubic Interpolation**

Figure 4.4 presents the MSE values for each method at a sampling rate of 20% with an SNR of -5 dB. The proposed sparse recovery method achieved the lowest MSE, outperforming the interpolation techniques, which struggled to accurately reconstruct the subsurface images under high noise and sparse sampling conditions.

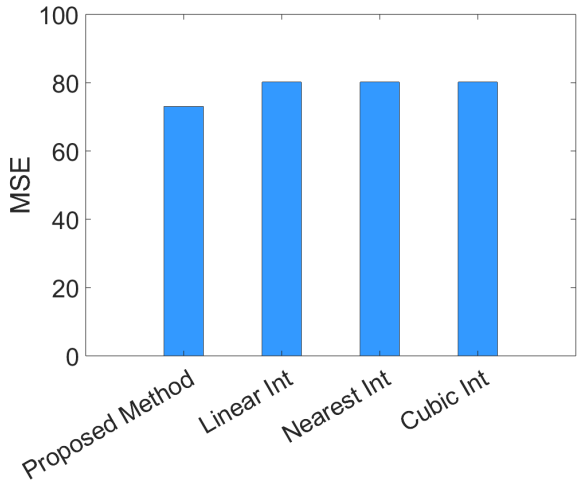

Figure 4.4: MSE comparison for 20% sampling with −5 dB noise across different data reconstruction methods: sparse recovery (proposed), linear interpolation, nearest neighbor interpolation, and cubic interpolation.

4.5 Effect of Cross-Validation Parameter α

The parameter α in the cross-validation procedure of the Dantzig Selector plays a crucial role in balancing sparsity and data fidelity. We investigated the effect of varying α on the reconstruction performance by analyzing the MSE for different α values ranging from 0.1 to 0.9.

Figure 4.5 illustrates the relationship between α and MSE for the case of 30% sampling with an SNR of -5 dB. The results indicate that lower α values generally lead to lower MSE, enhancing reconstruction accuracy by allowing more non-zero coefficients in the solution. However, excessively low α values may introduce noise and reduce sparsity.

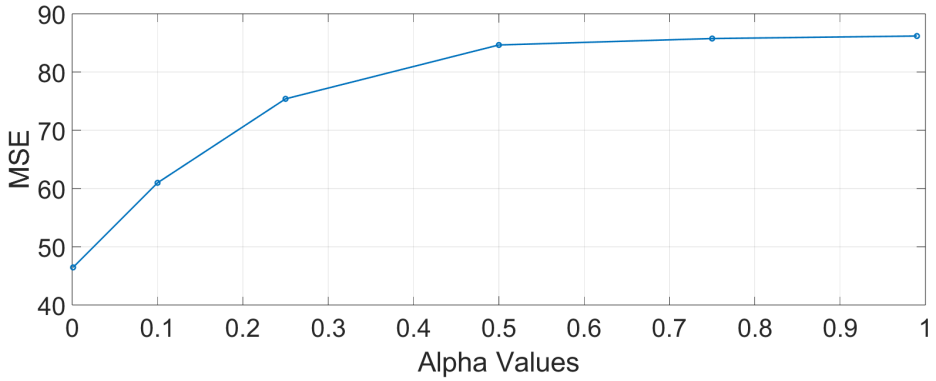

Figure 4.5: MSE versus cross-validation parameter α for 30% sampling with -5 dB noise. Lower α values improve reconstruction accuracy but may affect sparsity.

4.6 Discussion

4.6.1 Effectiveness of Sparse Recovery in GPR Imaging

The results demonstrate that the proposed sparse recovery framework effectively reconstructs high-quality 3D subsurface images from sparsely and irregularly sampled GPR data even in the noisy environment. By leveraging the inherent sparsity of the subsurface reflectivity, the method overcomes the limitations of traditional imaging techniques that rely on dense and regular sampling patterns.

4.6.2 Advantages over Traditional Methods

Compared to traditional interpolation methods, the sparse recovery framework provides superior reconstruction performance, especially under adverse conditions. The ability to accurately reconstruct missing data enables the use of conventional imag-

ing algorithms like BPA, resulting in high-resolution images without the need for extensive data acquisition.

4.6.3 Practical Implications

The flexibility to collect data along arbitrary paths and the reduction in required measurements significantly enhance the practicality of GPR surveys. This is particularly beneficial in complex environments with obstacles or accessibility constraints, where regular grid scanning is impractical.

4.7 Summary

In this chapter, we validated the proposed sparse recovery framework for enhancing 3D GPR imaging from sparsely and irregularly sampled data. Through simulations using gprMax, we demonstrated that the method effectively reconstructs missing data, enabling accurate subsurface imaging even under high noise levels and low sampling densities. The performance analysis confirmed the robustness and superiority of the sparse recovery approach over traditional interpolation methods. The impact of the cross-validation parameter α was examined, providing insights into the balance between sparsity and accuracy. Overall, the results underscore the potential of the proposed method to improve the efficiency and applicability of GPR surveys in real-world scenarios.

Chapter 5

Conclusion and Future Work

5.1 Conclusion

In this thesis, we investigated the application of sparse recovery techniques to enhance three-dimensional (3D) Ground Penetrating Radar (GPR) imaging from sparsely and irregularly sampled data collected along arbitrary scanning paths. Traditional GPR imaging methods require dense spatial sampling along regular grids, which is often impractical and time-consuming, especially in complex environments with obstacles or accessibility constraints. Our research addresses this challenge by developing a robust sparse recovery framework that leverages the inherent sparsity of subsurface features to reconstruct high-quality 3D images from reduced and irregularly sampled measurements.

The key contributions of this research are summarized as follows:

- **Development of a Sparse Recovery Framework for Arbitrary Path Scanning**: We proposed a sparse recovery framework utilizing the Dantzig

Selector formulation with cross-validation, specifically tailored for GPR data collected along arbitrary paths. This framework effectively reconstructs the sparse reflectivity of the subsurface, enabling accurate imaging without the need for regular grid sampling.

- **Demonstration of High-Quality 3D Imaging from Sparse and Irregular Data**: Through comprehensive simulations, we demonstrated that high-resolution 3D subsurface images can be reconstructed from sparsely and irregularly sampled data. Our method maintains imaging quality even at low sampling densities and in the presence of significant noise, outperforming traditional interpolation and imaging techniques.

- **Enhancement of Practicality and Efficiency in GPR Surveys**: By accommodating arbitrary scanning paths, our approach allows for flexible survey designs that can navigate around obstacles and adapt to challenging terrains. This significantly enhances the practicality and efficiency of GPR surveys in real-world scenarios where regular grid scanning is impractical or impossible.

- **Reduction in Data Acquisition and Processing Requirements**: The ability to reconstruct accurate 3D images from fewer measurements reduces the time and resources required for data collection and processing. This makes large-scale or time-sensitive GPR applications more feasible and cost-effective.

The findings of this research highlight the potential of sparse recovery techniques to transform 3D GPR imaging. By exploiting the sparsity of subsurface targets and accommodating arbitrary sampling patterns, we can significantly reduce data acquisition requirements and processing times while maintaining or even improving imaging

quality. This advancement opens up new possibilities for efficient subsurface exploration in complex environments, making GPR surveys more versatile and accessible.

5.2 Future Work

While the proposed method shows significant promise, several areas warrant further exploration:

- **Extension to Real-World Data**: Future research should focus on validating the framework with real-world GPR datasets collected in diverse environments to assess its practical performance and adaptability.
- **Integration with Adaptive Scanning Strategies**: Incorporating adaptive scanning paths based on preliminary survey results could further optimize data acquisition, focusing resources on areas of interest.
- **Algorithmic Enhancements**: Exploring advanced sparse recovery algorithms and incorporating machine learning techniques may enhance reconstruction accuracy and computational efficiency.
- **Handling Complex Subsurface Conditions**: Extending the framework to account for heterogeneous subsurface properties, such as varying dielectric constants and complex geological structures, would increase its applicability.

In conclusion, the integration of sparse recovery techniques with GPR imaging along arbitrary scanning paths represents a significant advancement in subsurface exploration technology. This research contributes to the development of more efficient,

flexible, and accurate GPR imaging methods, facilitating better decision-making in engineering, environmental studies, archaeology, and other fields requiring subsurface investigation.

5.3 Implications of the Research

The implications of this work are multifaceted, impacting both the theoretical and practical aspects of GPR imaging:

- **Advancement in 3D Sparse Signal Processing**: This research contributes to the field of sparse signal processing by extending the application of the Dantzig Selector to 3D data and arbitrary sampling patterns. It showcases the feasibility and benefits of applying advanced sparse recovery techniques in complex GPR imaging scenarios.
- **Enhanced GPR Survey Flexibility**: Practitioners can conduct GPR surveys more flexibly, designing arbitrary scanning paths that adapt to environmental constraints or specific areas of interest. This flexibility is particularly valuable in urban environments, rough terrains, or sites with obstacles.
- **Improved 3D Subsurface Imaging Quality**: The ability to reconstruct high-resolution 3D images from sparsely and arbitrarily sampled data enhances the detection and characterization of subsurface features. This improvement is critical in applications such as utility detection, archaeological exploration, and environmental monitoring, where volumetric information is essential.

- **Reduction in Data Acquisition and Processing Requirements**: By effectively handling arbitrary path scanning and reducing the number of required measurements, the proposed methods decrease both the time and resources needed for data collection and processing in 3D GPR imaging.
- **Potential for New Applications**: The advancements in arbitrary path and 3D imaging open up possibilities for new applications of GPR technology in areas previously considered challenging due to sampling constraints.

5.4 Future Work

While the research presented has made significant strides in improving GPR imaging through sparse recovery techniques, particularly in 3D and arbitrary path contexts, several avenues for future work remain:

5.4.1 Algorithm Optimization for Large-Scale 3D Imaging

The computational complexity of the Dantzig Selector in large-scale 3D imaging presents challenges. Future research can focus on:

- **Scalable Algorithms**: Developing algorithms that scale efficiently with the size of the 3D data, possibly through dimensionality reduction techniques or hierarchical processing.
- **Parallel Computing and High-Performance Computing (HPC)**: Lever-

aging HPC resources, such as multi-core processors, GPUs, or distributed computing environments, to handle the computational demands of 3D sparse recovery.

- **Algorithmic Approximation**: Investigating approximate algorithms that offer a balance between computational efficiency and reconstruction accuracy in 3D contexts.

5.4.2 Integration with Machine Learning Techniques

Combining sparse recovery with machine learning can lead to improved performance and new capabilities:

- **Deep Learning for 3D Reconstruction**: Applying deep learning models to learn complex mappings from arbitrarily sampled data to full-resolution 3D images, potentially enhancing reconstruction quality and speed.
- **Data-Driven Parameter Optimization**: Using machine learning to automatically select or tune algorithm parameters based on the characteristics of the data, improving robustness and ease of use.
- **Feature Extraction and Classification**: Integrating feature extraction and classification tasks into the reconstruction process, enabling automated interpretation of 3D GPR images.

5.4.3 Field Validation in Diverse Environments

Extending field validation efforts to a wider range of environments will strengthen the applicability of the methods:

- **Testing in Complex Terrains**: Conducting field tests in environments with challenging conditions, such as uneven terrain, urban areas with significant clutter, or sites with variable subsurface properties.
- **Longitudinal Studies**: Performing repeated surveys over time to assess the methods' performance in monitoring applications, such as detecting changes in subsurface structures or tracking environmental processes.
- **Cross-Disciplinary Collaboration**: Working with experts from geology, archaeology, civil engineering, and other fields to apply the methods to real-world problems and gather diverse feedback.

5.4.4 Real-Time 3D Imaging and Visualization

Developing capabilities for real-time 3D imaging and visualization will enhance the practicality and user experience:

- **Onboard Real-Time Processing**: Implementing the algorithms on embedded systems within GPR equipment to provide immediate 3D imaging results during surveys.
- **Advanced Visualization Tools**: Creating interactive visualization platforms

that allow users to explore 3D subsurface images in real-time, potentially incorporating augmented reality (AR) or virtual reality (VR) technologies.

- **User Interface Design**: Designing intuitive interfaces that enable practitioners to easily interpret and interact with 3D imaging data collected along arbitrary paths.

5.4.5 Extension to Multi-Modal Imaging Systems

Exploring the integration of GPR with other sensing modalities can provide comprehensive subsurface characterization:

- **Data Fusion Techniques**: Developing methods to combine GPR data with data from other sensors, such as electromagnetic induction, seismic, or optical sensors, enhancing the reliability and richness of subsurface information.
- **Joint Inversion Methods**: Creating algorithms that jointly invert data from multiple modalities to improve resolution and reduce ambiguities in subsurface imaging.
- **Cross-Calibration and Alignment**: Addressing challenges related to aligning and calibrating data from different sensors, especially when collected along arbitrary paths.

5.5 Final Remarks

The research undertaken in this thesis has demonstrated the significant potential of applying the Dantzig Selector and sparse recovery techniques to 3D GPR imaging

with arbitrary path scanning. By addressing key challenges associated with data acquisition, sampling flexibility, and image reconstruction in three dimensions, the work contributes valuable insights and tools to the field of subsurface exploration. Continued efforts in this direction promise to further enhance the capabilities and applications of GPR technology, leading to more efficient, flexible, and accurate subsurface investigations in a wide range of environments and applications.

Bibliography

[1] Daniels, D.J. (2004). Ground Penetrating Radar (2nd ed.). IET.

[2] H. M. Jol, “Ground Penetrating Radar Theory and Applications,“ Elsevier, 2008.

[3] J. M. Reynolds, “An Introduction to Applied and Environmental Geophysics,“ 2nd ed., John Wiley & Sons, 2011.

[4] M. Pereira, D. Burns, D. Orfeo, Y. Zhang, L. Jiao, D. Huston, and T. Xia, “3-D multistatic ground penetrating radar imaging for augmented reality visualization,“ *IEEE Transactions on Geoscience and Remote Sensing*, vol. 58, number 8, pp. 5666-5675, 2020.

[5] O. Yilmaz, “Seismic Data Analysis: Processing, Inversion, and Interpretation of Seismic Data,“ Society of Exploration Geophysicists, Tulsa, OK, 2001, 1028 p. Available: https://doi.org/10.1190/1.9781560801580

[6] N. Smitha, D. R. Ullas Bharadwaj, S. Abilash, S. N. Sridhara, and V. Singh, “Kirchhoff and F-K migration to focus ground penetrating radar images,” *Geo-Engineering*, vol. 7, no. 4, 2016. [Online]. Available: https://doi.org/10.1186/s40703-016-0019-6

[7] X. Feng, M. Sato, “Pre-stack migration applied to GPR for landmine detection,“ Inverse Problems 20 (2004) 99-115.

[8] J. I. Halman, K. A. Shubert, and G. T. Ruck, "SAR processing of ground-penetrating radar data for buried UXO detection: Results from a surface-based system," *IEEE Trans. Antenn. Propag.*, vol. 46, 1998, pp. 1023-1027. [CrossRef]

[9] R. Zetik, J. Sachs, and R. Thoma, "Modified cross-correlation back projection for UWB imaging: Numerical examples," in *Proceedings of the IEEE International Conference on Ultra-Wideband*, Zurich, Switzerland, 5-8 September 2005.

[10] L. Qu and Y. Yin, "Nonuniform fast Fourier transform-based fast back-projection algorithm for stepped frequency continuous wave ground penetrating radar imaging," *J. Appl. Remote Sens.*, vol. 10, 2016, Art. no. 45009. [CrossRef]

[11] M. Cheney and B. Borden, "Fundamentals of Radar Imaging," SIAM, 2009.

[12] A. C. Gurbuz, J. H. McClellan, and W. R. Scott, "Compressive sensing for subsurface imaging using ground penetrating radar," *Signal Processing*, vol. 89, no. 10, pp. 1959-1972, 2009.

[13] E. Candes, J. Romberg, and T. Tao, "Stable signal recovery from incomplete and inaccurate measurements," *Comm. on Pure and Applied Math.*, vol. 59, no. 8, pp. 1207–1223, 2006.

[14] D. L. Donoho, "Compressed sensing," *IEEE Trans. Inf. Theory*, vol. 52, no. 4, pp. 1289-1306, Apr. 2006.

[15] A. C. Gurbuz, J. H. McClellan, and W. R. Scott, "Compressive Sensing for GPR Imaging," 2007 Conference Record of the Forty-First Asilomar Conference on Signals, Systems and Computers, Pacific Grove, CA, USA, 2007, pp. 2223-2227, doi: 10.1109/ACSSC.2007.4487636.

[16] M. Herman and T. Strohmer, "High-Resolution Radar via Compressed Sensing," *IEEE Transactions on Signal Processing*, vol. 57, pp. 2275-2284, 2009. Available: https://doi.org/10.1109/TSP.2009.2014277

[17] Y. Zhang, and T. Xia, "Frequency domain clutter removal for compressive OFDM ground penetrating radar," *IEEE International Symposium on Circuits and Systems (ISCAS)* 2016.

[18] H. Frigui, L. Zhang, P. Gader, J. N. Wilson, K. C. Ho, and A. Mendez-Vazquez, "An evaluation of several fusion algorithms for anti-tank landmine detection and discrimination," *Information Fusion*, vol. 13, no. 2, pp. 161-174, 2012. Available: https://doi.org/10.1016/j.inffus.2009.10.001

[19] E. J. Candes and T. Tao, "The Dantzig selector: Statistical estimation when p is much larger than n," *Annals of Statistics*, vol. 35, no. 6, pp. 2313-2351, 2007.

[20] A. F. Yegulalp, "Fast backprojection algorithm for synthetic aperture radar," *Proceedings of the 1999 IEEE Radar Conference. Radar into the Next Millennium (Cat. No.99CH36249)*, Waltham, MA, USA, 1999, pp. 60-65. doi: 10.1109/NRC.1999.767270.

[21] C. Warren, A. Giannopoulos, and I. Giannakis, "gprMax: Open source software to simulate electromagnetic wave propagation for Ground Penetrating Radar," *Computer Physics Communications*, vol. 209, pp. 163–170, 2016, doi: 10.1016/j.cpc.2016.08.020.

[22] M. Grant and S. Boyd, "CVX: Matlab Software for Disciplined Convex Programming, version 2.1," Available: https://cvxr.com/cvx, Mar. 2014.

Appendix A
Additional Resources

The source code developed during this research is openly available at:
https://github.com/nad1/BPAandSparseRecovery